Desalination and Water Treatment
www.deswater.com
doi: 10.5004/dwt.2020.25912

195 (2020) 87–95
August

Effect of rotor area covered by end cover on flow characteristics and performance of seawater desalination energy recovery device

Guangfei Ma[a,b,c], Zhe Lin[a,*], Zuchao Zhu[a], Yu Zheng[b], Yong Fang[b]

[a]*National Joint Engineering Laboratory of fluid transfer system, Zhejiang Sci-Tech University, Hangzhou 310018, China, emails: linzhe0122@zstu.edu.cn (Z. Lin), maguangfei@126.com (G. Ma), zhuzuchao@zstu.edu.cn (Z. Zhu)*
[b]*Standard and Quality Control Research Institute, Ministry of Water Resources and Hangzhou Machine Design and Research Institute, Ministry of Water Resources, Hangzhou 310012, China, emails: solomon128@126.com (Y. Zheng), fangyongshuilibu@126.com (Y. Fang)*
[c]*Key Laboratory of Fluid and Power Machinery (Xihua University), Ministry of Education, Chengdu 610039, China*

Received 3 September 2019; Accepted 25 March 2020

ABSTRACT

The multi-phase flow mixing numerical model was used to simulate the influence of the end cover on the rotor area on the flow characteristics and performance of the seawater desalination energy recovery device under three structural designs. The pressure energy recovery efficiency, flow field pressure distribution, and NaCl concentration distribution, high pressure inlet, and outlet differential pressure characteristics, and pressure pulsation characteristics of seawater desalination energy recovery device were numerically simulated under different end caps covering rotor area and speed. The results show that the area covered by the end face of the rotor plays an important role in the recovery efficiency of the pressure energy. The effect of rotational speed on the recovery efficiency of the pressure energy is not uniquely determined, but there is a rotational speed in which the rotor speed is not suitable for the energy recovery efficiency. The higher the pressure difference between the high pressure inlet and outlet of the energy recovery device, the lower the pressure energy recovery efficiency. Considering the fluid-forming hydrostatic mechanical seal and system stability, the design method of the structure *a* (single layer, area = 3,534.29 mm^2) end cover covering the rotor area is the optimal design among the three structures.

Keywords: End cap covering rotor area; Rotor speed; Energy recovery efficiency; Pressure fluctuation at high pressure inlet and outlet; Numerical simulation

1. Introduction

Seawater is one of the most important resources. Seawater utilization is considered as an important solution to the shortage of water resources in coastal countries and regions. It is also an essential supplement and strategic reserve of water resources in coastal areas. At present, the research of seawater desalination technology mainly includes reverse osmosis, low-temperature multi-effect, multistage flash evaporation, electrodialysis, pressure steam distillation, dew point evaporation, hydropower co-generation, hot-film co-generation, and the utilization of river energy, solar energy, wind energy, tidal energy, and so on. From the perspective of large classification, it can be divided into two main classes: distillation (thermal method) and membrane method, among which low-multi-effect distillation, multistage flash distillation and reverse osmosis membrane method are the mainstream technologies in the world [1–4]. Therefore, the research and development of seawater utilization of new products, new processes, and new technologies, conforming with sustainable development strategy were proposed.

By reviewing and analyzing related literature at home and abroad, it can be found that reverse osmosis desalination

* Corresponding author.

technology has become the mainstream technology of market choice because of its advantages of low energy consumption, low investment cost and high service life of the equipment. In the reverse osmosis desalination system, the high-pressure raw seawater still has higher high-pressure energy (called high-pressure concentrated seawater) after it passes through the reverse osmosis membrane. How to efficiently utilize the residual pressure energy in high-pressure concentrated seawater and design a reasonable energy recovery device for seawater desalination is an important goal for scientific researchers and enterprises at home and abroad to tackle key problems in science and technology. At present, the devices for utilizing the residual high-pressure energy in desalination are called energy recovery devices or pressure energy exchange devices. They mainly include "self-transformation rotary energy exchange device," "external drive rotary energy exchange device," "power exchange energy recovery device," "pump-motor energy recovery device" and "turbine," pressure energy recovery device of the supercharged pump, and so on [5–11]. Among them, "rotary energy exchange device" has high efficiency of pressure energy recovery, but its pressure energy recovery technology has the characteristics of complexity and strict technical confidentiality. There are few detailed research materials published on core technical issues. Therefore, structural design and process difficulty play an important role in its energy conversion efficiency.

In recent years, domestic and foreign scholars have adopted the computational fluid dynamics (CFD) method to explore more and more important issues in desalination technology based on different turbulence models and two-phase flow models. Mainly, Yang et al. [12] simulated the desorption rate of CO_2 in the actual seawater desalination system and its influencing factors by establishing a mathematical model of CO_2 chemical desorption in a multi-effect evaporation desalination system. Xu et al. [13] used CFD simulation and verification experiments to study the calculation theory of the rotor speed of a self-driven rotary energy recovery device. Dimitriou et al. [14] presented an experimental comparison between two small-scale SWRO units equipped with different energy recovery devices determine to lower the specific energy consumption. Li et al [15] made use of the response surface method to simulate a standard seawater desalination system to optimize the membrane flux of the desalination system. Qureshi and Zubair [16] investigated various energy recovery devices for a brackish water reverse osmosis desalination unit based on second-law analysis coupled with specific energy consumption calculations. They found the suggested second-law efficiency with specific energy consumption with their product and obtained a simple function of the permeate density and specific exergy. Liu et al. [17] used computational fluid dynamics to analyze the leakage characteristics of valve-controlled seawater desalination energy recovery and explored the relationship between leakage characteristics and efficiency and performance. Qi et al. [18] used the combination of the CFD method and experimental measurement to study the internal leakage of the pilot-scale fluid switching energy recovery device in the reverse osmosis system. There are still many studies related to seawater desalination technology, and the article does not appear.

Therefore, based on Fluent software, a three-dimensional numerical simulation of the transient characteristics of the self-designed desalination energy recovery device is carried out in this paper. Based on the sliding moving grid technology, the influence of end coverage area and the number of rows of rotor channels on the pressure energy exchange efficiency and internal flow characteristics of desalination energy recovery device were studied.

2. Numerical calculation method

2.1. Physical model

This paper mainly studies the influence of the end cover covering the rotor area on the flow field characteristics and pressure energy exchange efficiency in the seawater desalination energy recovery device. The basic model of the three-dimensional structure of the energy recovery device is illustrated in Fig. 1. The length of the upper and lower end caps is l = 30 mm, and the diameter of the indexing circle is D = 100 mm. The internal flow passages are unified in the sleeve as the rotor structure of the energy recovery device. There are different numbers of flow passages inside the rotor, and the length of the sleeve is L = 300 mm. The high-pressure inlet and low-pressure outlet, low-pressure inlet, and high-pressure outlet are located inside the upper and lower end caps, respectively. It is also called a collecting tank. The length and diameter are based on the processing capacity of some islands.

2.2. Mathematical model

In this paper, the CFD method is used to study the internal flow field characteristics and pressure energy exchange efficiency of the self-designed desalination energy recovery device. Considering the complexity of the flow field under high pressure, the turbulence characteristics of the flow and the incompressibility of the liquid are taken into account. In order to fit the actual working conditions, a two-fluid model was used to treat high and low concentration seawater.

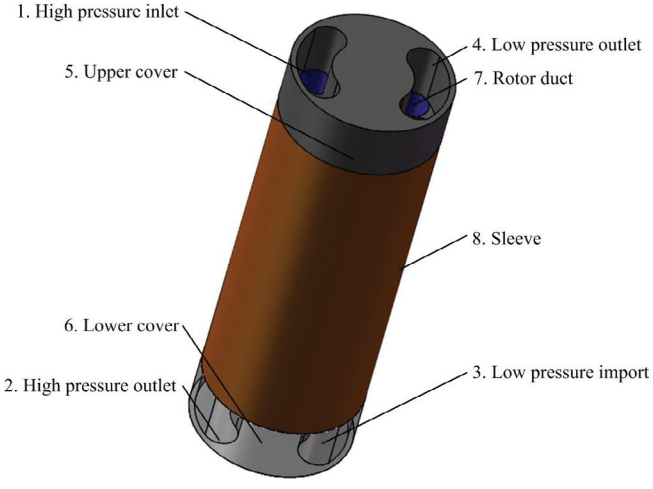

Fig. 1. Three-dimensional structure model of seawater desalination energy recovery device.

The mathematical models include continuity equation [19], momentum equation, standard k-ε two-equation turbulence model [20,21] and mixture model [22,23].

The governing equations of mixture model mainly include:

(1) Mixed continuity equation:

$$\frac{\partial \rho_m}{\partial t} + \nabla\left(\rho_m u_m\right) = 0 \tag{1}$$

$$u_m = \frac{\sum_{k=1}^{n} \alpha_k \rho_k u_k}{\rho_m} \tag{2}$$

$$\rho_m = \sum_{k=1}^{n} \alpha_k \rho_k \tag{3}$$

where u_m is the average velocity of the mixed phase; ρ_m represents the density of the mixed phase; α_k is the volume fraction of the k phase.

(2) Mixed momentum equation:

$$\frac{\partial}{\partial t}(\rho_m u_m) + \nabla(\rho_m u_m u_m) = -\nabla P + \nabla\left[\mu_m\left(\nabla u_m + \nabla u_m^T\right)\right] + \rho_m g + F + \nabla\left[\sum_{k=1}^{n} \alpha_k \rho_k u_{dr,k} u_{dr,k}\right] \tag{4}$$

$$\mu_m = \sum_{k=1}^{n} \alpha_k \mu_k \tag{5}$$

where n is the number of phases (n = 2); F is the volumetric force; g is the gravitational acceleration; μ_m is the mixed viscosity coefficient; $u_{dr,k}$ is the drift velocity of the second phase k, $u_{dr,k} = u_k - u_m$.

(3) k-ε turbulence model:

$$\frac{\partial\left(\rho k\right)}{\partial t} + \frac{\partial\left(\rho u_j k\right)}{\partial x_j} = \frac{\partial}{\partial x_i}\left[\left(\mu + \frac{\mu_t}{\sigma_k}\right)\frac{\partial k}{\partial x_i}\right] + \mu_t \frac{\partial u_i}{\partial x_j}\left(\frac{\partial u_i}{\partial x_j} + \frac{\partial u_j}{\partial x_i}\right) - \rho\varepsilon \tag{6}$$

$$\frac{\partial\left(\rho\varepsilon\right)}{\partial t} + \frac{\partial\left(\rho u_j \varepsilon\right)}{\partial x_j} = \frac{\partial}{\partial x_i}\left[\left(\mu + \frac{\mu_t}{\sigma_\varepsilon}\right)\frac{\partial \varepsilon}{\partial x_i}\right] + \frac{C_1 \varepsilon}{k}\mu_t \frac{\partial u_i}{\partial x_j}\left(\frac{\partial u_i}{\partial x_j} + \frac{\partial u_j}{\partial x_i}\right) - C_2 \rho \frac{\varepsilon^2}{k} \tag{7}$$

In Eqs. (6) and (7), k and ε represent the turbulent flow energy and turbulent dissipation rate, respectively; μ_t is the turbulent viscosity; C_1, C_2, σ_k, and σ_ε are the constants obtained experimentally. C_1 = 1.44, C_2 = 1.92, σ_k = 1.0, σ_ε = 1.3.

2.3. Computing objects and mesh generation

In order to study the influence of end cover covering rotor area and number of rows of rotor channels on pressure energy exchange efficiency and internal flow characteristics of seawater desalination energy recovery device. On the basic structure of Fig. 1, this paper designs three types of energy recovery devices for desalination with a rotor area coverage structure. The flow channel structure is shown in Fig. 2. The results that the coverage area of the rotor passage and the specific structural parameters are listed in Table 1.

Since all three structures adopt a structured computational grid to carry out three-dimensional numerical simulation of the whole flow field, this paper only gives the grid division of one model structure, as shown in Fig. 3.

2.4. Boundary conditions

Inlet boundary condition setting: velocity inlet. Based on the actual operating conditions of a desalination plant, the high pressure and low pressure inlet speed values are given according to the design flow rate (Q = 55 m^3/h).

The flow velocity at the inlet and outlet can be calculated by the design flow, $Q = A \times v$, $v = Q/A$; where, Q is the design flow, A is the section area of the end cover hole, v_1, v_2, and v_3 are the inlet speeds of three structures, respectively.

v_1 = 4.32 m/s, v_2 = 5.89 m/s, v_3 = 6.07 m/s.

Outlet boundary condition setting: pressure outlet. According to the actual operation conditions of a desalination plant, the high-pressure outlet pressure value P = 5 Mpa and the low-pressure outlet pressure value P = 0 Mpa.

Rotor speed: 600–1,600 rpm. Five typical rotational speeds were selected for the study, namely 600; 800; 1,000; 1,200; 1,400; and 1,600 rpm.

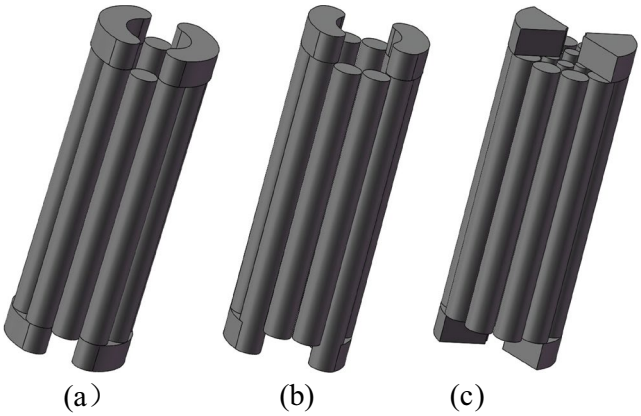

Fig. 2. Three rotor channel area covering structure.

Table 1
Coverage area and specific structural parameters of the rotor

Ordinal number	*a*	*b*	*c*
Area (mm^2)	3,534.29	2,591.81	2,516.55
Channel layer/layer	1	1	2
Outer diameter (mm)	30	30	30
Number of outer holes	10	10	10
Inner diameter (mm)	/	/	18
Number of inner holes	/	/	6

Fig. 3. Schematic diagram of model structure meshing parameters of the rotor.

The speed determines the efficiency of pressure exchange and the mixing rate when the medium contacts. It is an important parameter of the rotary pressure exchanger. The rotor speed varies from 500 to 2,000 rpm according to the flow rate [24]. However, because the rotating pressure exchanger is a high-pressure closed vessel, the rotor rotates in the vessel, in this case, the traditional speed measurement methods are all invalid, so the measurement of the internal rotor speed of the pressure exchanger is a big difficulty. Therefore, this paper uses the speed range of references to study the performance of the external force driven energy recovery device.

The high pressure inlet is high concentration brine (equivalent to high concentration seawater after reverse osmosis membrane), NaCl concentration is 0.035, density is 1.02478 kg/m^3.

The low pressure inlet is low concentration brine (equivalent to raw seawater), NaCl concentration is 0.018, density is 1.021342 kg/m^3. The calculated temperature is 298 K.

Because there are three structures and multiple rotating speeds in the numerical simulation of the desalination energy recovery device, in order to make better numerical comparison, the numerical simulation time step is set to 0.001 s, the iteration calculation is done at 1,000 steps, and the convergence residual is 10^{-6}. During the calculation, the pressure and flow on the high-pressure inlet and outlet sections are monitored dynamically.

The flow is obtained by monitoring the flow on the end cover section.

By reading the references, the gap between the end cover and the rotor is 0.01–0.025 mm, which is the most efficient. The gap is very small, this study does not consider the impact of gap, the impact of gap on it can be ignored [11,13,24].

3. Results and discussion

3.1. Pressure energy recovery efficiency

The efficiency of pressure energy recovery and conversion of desalination energy recovery device is an important goal for scientific researchers and enterprises at home and abroad to tackle key problems in science and technology. The current definition of recovery efficiency for energy recovery devices [5,9] is as follows:

$$\eta = \frac{Q_{\text{hpout}} \times P_{\text{hpout}} + Q_{\text{lpout}} \times P_{\text{lpout}}}{P_{\text{hpin}} \times Q_{\text{hpin}} + P_{lpin} \times Q_{\text{lpin}}} \tag{8}$$

where η represents the pressure energy recovery efficiency of the seawater desalination energy recovery device; P_{hpout} and P_{lpout} represent the pressure values of the high pressure and low pressure outlets, respectively, (Pa); P_{hpin} and P_{lpin} represent the pressure values of the high pressure and low pressure inlets, respectively, (Pa); Q_{hpout} and Q_{lpout} represent the volume flow values of the high and low pressure outlets, respectively, (m^3/h); Q_{hpin} and Q_{lpin} represent the flow values of the high pressure and low pressure inlets, respectively, (m^3/h).

The pressure energy recovery efficiency chart of the desalination energy recovery device is shown in Fig. 4 under three structural forms at different rotating speeds after the mean treatment. It can be seen from Fig. 4 that under given design flow rate Q, (1) When rotating speed n = 600–1,200 rpm, structure a (single layer, area = 3,534.29 mm^2) has the greatest recovery efficiency of pressure energy. That is to say, the larger the area of end cover covering the rotor channel, the greater the recovery efficiency of pressure energy, structure b (single layer, area = 2,591.81 mm^2) has the same trend of pressure energy recovery efficiency as structure a; the pressure energy recovery efficiency of structure c (double layer, area = 2,516.55 mm^2) decreases first and then increases (2). When the speed is n = 1,200–1,600 rpm, the pressure energy recovery efficiency of structure a (single layer, area = 3,534.29 mm^2) decreases first, then increases slightly, and finally continues to decrease; there is a large increasing trend of the pressure energy recovery efficiency of structure b (single layer, area = 2,591.81 mm^2); the pressure energy recovery efficiency of structure c (double layer, area = 2,516.55 mm^2) shows a decreasing trend (3). In the process of rotational speed n = 1,000–1,600 rpm, the overall efficiency of structure a (single layer, area = 3,534.29 mm^2) decreases first, then increases and then decreases; structure b (single layer, area = 2,591.81 mm^2), its overall efficiency decreases first and then increases; the overall efficiency of structure c (double layer, area = 2,516.55 mm^2) is reduced first, then increased, and then decreased (4). The efficiency of structure a (single layer, area = 3,534.29 mm^2) is the highest when rotational speed n = 600–1,200 rpm. The change of pressure energy recovery efficiency is only related to the respective structural design under the three structural designs, without cross regularity, but there

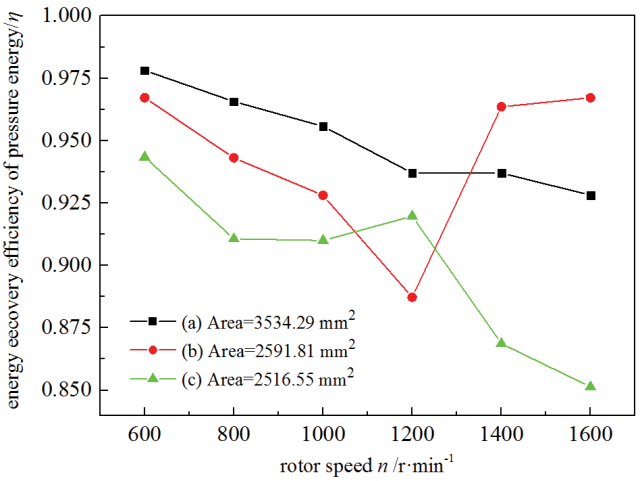

Fig. 4. Rotating speed (n)-efficiency (η) under different structures.

are rotating speeds with the same recovery efficiency at the speed n = 1,200–1,600 rpm. When the rotating speed n = 1,200 rpm, the pressure energy recovery efficiency of the three structures changes simultaneously.

Through the above analysis, it can be shown that under the given design flow, the area of the end cover rotor passage plays an important role in the efficiency of pressure energy recovery, and the unreasonable coverage area makes the efficiency of pressure energy recovery very low, which cannot meet the design requirements. At the same time, the influence of rotating speed on the efficiency of pressure energy recovery is not unique, but there is a rotating speed that does not adapt to the efficiency of energy recovery.

3.2. Pressure field distribution inside the energy recovery device

Through energy recovery efficiency analysis conducted in section 3.1 (Pressure energy recovery efficiency), the study found that the effect of rotational speed on the energy recovery efficiency mainly occurs at the rotor speed n = 1,200; 1,400 rpm, and n = 1,200 rpm is the lowest efficiency point in the turning point of the energy recovery efficiency change of the three structural design methods. Therefore, this paper focuses on the three-dimensional flow field pressure distribution in the energy recovery device when the rotor speed is n = 1,200 rpm.

Fig. 5. shows the pressure nephogram distribution of flow field in the energy recovery device with structure a (single layer, area = 3,534.29 mm²), b (single layer, area = 2,591.81 mm²), and c (double layer, area = 2,516.55 mm²) at the same speed, calculation time and design flow rate. As can be seen from Fig. 5, under given design flow rate, pressure exchange (that's pressure energy recovery conversion) is accomplished in structures a, b, and c. High and low pressures are distributed in the rotor pipes of corresponding high and low pressure energy recovery devices respectively. Structure c (double layer, area = 2,516.55 mm²) has a maximum pressure of 5.357 × 10⁶ Pa and a minimum pressure difference, which indicates that the pressure loss is the smallest. Therefore, its energy recovery efficiency is higher than that of structure a and b. This also explains the reason why the energy recovery efficiency performance curve is more efficient when rotating speed n = 1,200 rpm.

3.3. Pressure recovery device high pressure inlet and outlet differential pressure characteristics

In section 3.2 (Pressure field distribution inside the energy recovery device), this paper analyzes the internal flow field pressure cloud map distribution of the energy recovery device under three structural designs. However, the overall pressure cloud diagram is difficult to explain the reason why the energy recovery efficiency turns when the rotor speed changes. Therefore, in order to better analyze the influence of the structural design on the energy recovery (conversion) efficiency of the energy recovery device. In this section, the average pressure difference of the high

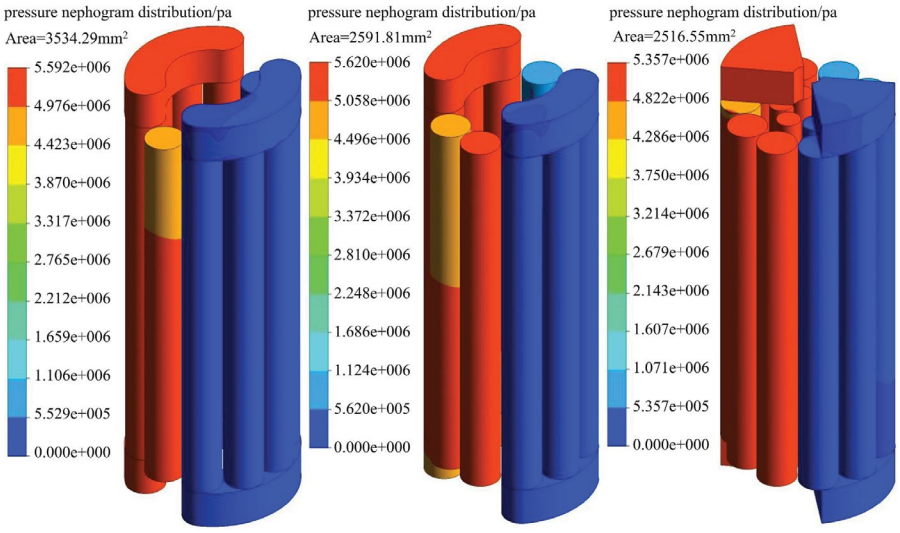

Fig. 5. Pressure nephogram distribution of flow field in energy recovery device.

pressure inlet and outlet of the energy recovery unit is analyzed under three structural design methods.

Fig. 6 is a diagram showing the rotational speed-pressure difference of the high-pressure inlet and outlet of the energy recovery device under different structural designs. As can be seen from Fig. 6, the pressure loss of the high pressure inlet and outlet is similar to the pressure energy recovery (conversion) efficiency of the energy recovery device. At the speed n = 1,200 rpm, the structure b (single layer, area = 2,591.81 mm^2) has the largest pressure loss, so its efficiency at this speed is the lowest.

At the same time, it can be seen from Fig. 6, that the pressure difference distribution at the high pressure inlet and outlet is opposite to the pressure energy recovery (conversion) efficiency distribution of the energy recovery device. This demonstrates that the greater the pressure difference between the high pressure inlet and outlet of the energy recovery device, the lower the efficiency of pressure energy recovery (conversion). Reducing the pressure loss at the high pressure inlet and outlet is the key technology to improve the pressure energy recovery (conversion) efficiency of the energy recovery device.

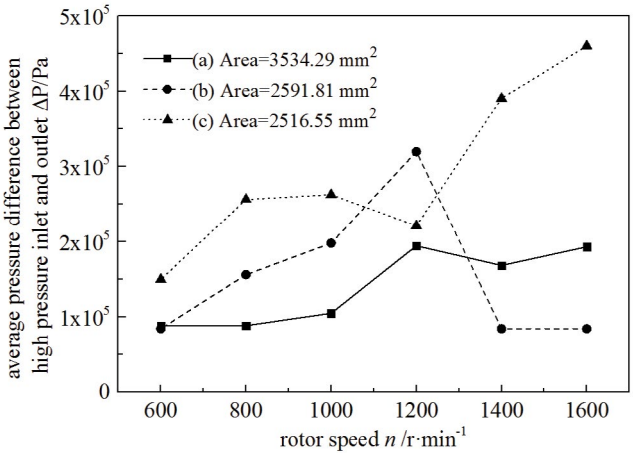

Fig. 6. Rotating speed (n)-pressure difference (ΔP) under different structure between high pressure inlet and outlet.

3.4. Energy recovery device high pressure inlet and outlet pressure pulsation

The reliability is related to the pressure fluctuation in time domain and frequency domain, which has been analyzed in this paper. With the operation time, the reliability of the hydrostatic mechanical seal formed by the end cover and the rotor passage decreases, which is easy to cause static and dynamic interference, and is not conducive to the stability of the energy recovery device system of desalination. It is involved in many fields to judge the sealing reliability by time–frequency characteristics.

Based on the analysis of sections 3.1 (Pressure energy recovery efficiency) and 3.3 (Pressure recovery device high pressure inlet and outlet differential pressure characteristics), it can be known that n = 1,200 rpm, and the energy recovery efficiency and the pressure difference characteristics of the high-pressure inlet and outlet are severely changed in the three structural design methods. Therefore, this paper focuses on the analysis of the pressure pulsation of the high-pressure inlet and outlet of the energy recovery device when the rotor speed n = 1,200 rpm.

Fig. 7 is a pressure pulsation time-domain diagram of the high pressure inlet of the energy recovery device under different structural design when n = 1,200 rpm. It can be seen from Fig. 7, that structure c (double layer, area = 2,516.55 mm^2), the inlet pressure has the largest change with the running time, and the pulsation degree is the strongest, which indicates that the pressure recovery of the energy recovery device is satisfied. Under the premise of efficiency, the design method of the structure c-end cover covering the rotor hole area, the reliability of the hydrostatic mechanical seal formed by the end cover and the rotor hole is reduced, which is easy to cause dynamic and static interference, which is not conducive to

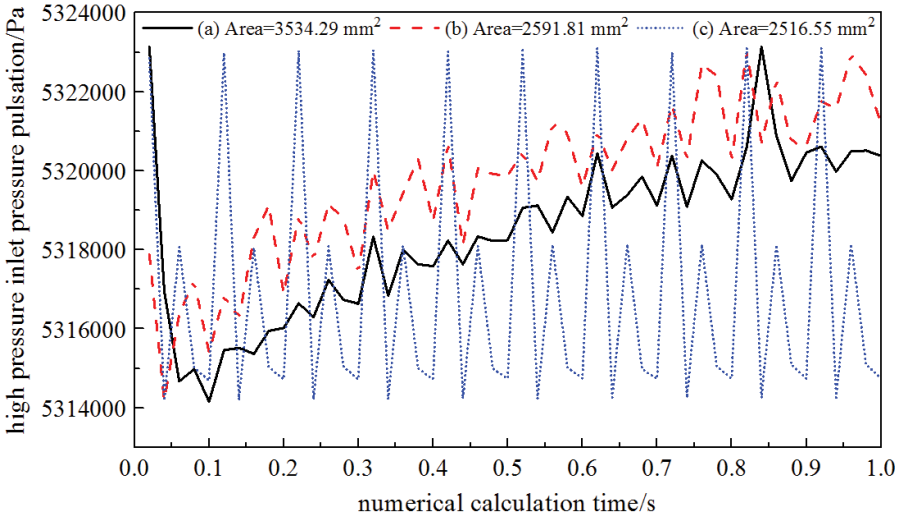

Fig. 7. n = 1,200 rpm, time domain diagram of pressure fluctuation at high pressure inlet under different structures.

the stability of the seawater desalination energy recovery device system. The design method of the structure *a* (single layer, area = 3,534.29 mm²) and the structure *b* (single layer, area = 2,591.81 mm²) cover the rotor area, the inlet pressure has the same trend with the running time, and the pulsation degree is the smallest. This shows that under the premise of satisfying the pressure energy recovery efficiency of the energy recovery device, the design method of covering the rotor area with the end caps of structure *a* and *b*, the hydrostatic mechanical seal of the end cap and the rotor is strong, and it is not easy to cause dynamic and static interference. Conducive to the stability of the seawater desalination energy recovery device system. Owing to the relative movement of the end cap and the rotor of the energy recovery device, it is necessary to consider the fluid to form a hydrostatic mechanical seal, and the pressure pulsation should be considered to be the minimum. Therefore, the design method of the structure *a* end cover covering the rotor area is the most excellent design.

Fig. 8. shows the pressure fluctuation spectrum of the high-pressure inlet of the energy recovery unit under different structural designs when n = 1,200 rpm.

To investigate the pressure fluctuation spectrum of the high-pressure inlet of the energy recovery unit under different structural designs, we studied the frequency spectrum at n = 1,200 rpm, as shown in Fig. 8. As can be seen from Fig. 8, structure *c* (double layer, area = 2,516.55 mm²) has the largest peak value at frequencies of 10 and 20 Hz. Structural *b* (single layer, area = 2,591.81 mm²) that the amplitude of peak value is the second, and the frequency is 20 Hz. Three kinds of structural design, high pressure inlet pressure fluctuation spectrum have certain periodicity. Among them, structure *a* (single layer, area = 3,534.29 mm²) has the lowest peak value on the whole, which shows that the end cover rotor area gets an impact on the stability of the desalination energy recovery device. Reasonable design of the end cover rotor area of the desalination energy recovery device can reduce the dynamic and static interference between the end cover and the rotor sealing surface, and improve the system stability.

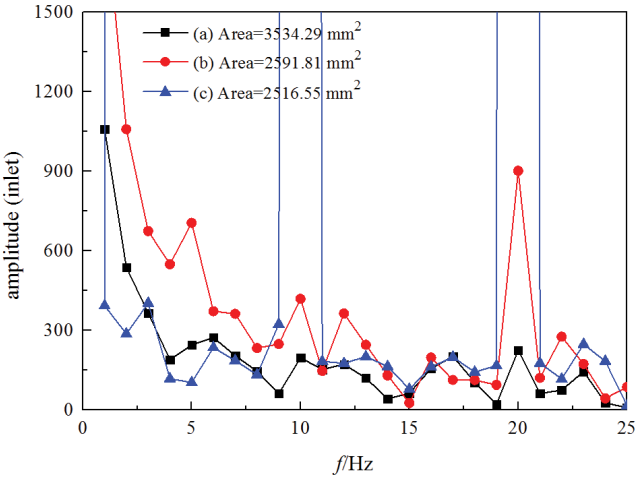

Fig. 8. n = 1,200 rpm, frequency spectrum of pressure fluctuation at high pressure inlet under different structures.

Fig. 9 shows the pressure fluctuation time-domain diagram of the high-pressure outlet of the energy recovery unit under different structural designs when n = 1,200 rpm.

It can be seen from Fig. 9, that the outlet pressure of structure *a* (single layer, area = 3,534.29 mm²) has the smallest change amplitude and the strongest pulsation degree with the operation time, which shows that under the premise of meeting the pressure energy recovery efficiency of the energy recovery device, the design method of covering the rotor area with the end cover of structure *a* has the highest reliability of forming the hydrostatic mechanical seal between the end cover and the rotor, which is not easy to cause dynamic and static interference is beneficial to the stability of the energy recovery system of desalination. Structure *c* (double layer, area = 2,516.55 mm²), the change

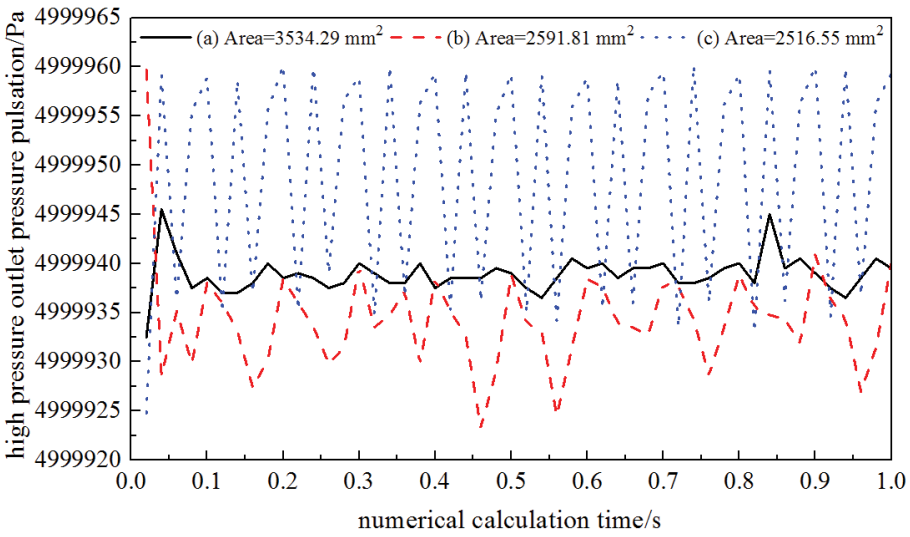

Fig. 9. n = 1,200 rpm, time domain diagram of pressure fluctuation at high pressure outlet under different structures.

range of outlet pressure with operation time is still the largest, and the fluctuation degree is the strongest, which has the greatest impact on the stability of the desalination energy recovery device system. Although structural *b* (single layer, area = 3,534.29 mm^2) outlet pressure changes little with the operation time, the high-pressure outlet pressure of the desalination energy recovery device is still quite large, and there is still a high-intensity pulsation. In conclusion, the design method of covering rotor area with end cover of structure *a* is the optimal design among the three structures.

Fig. 10 is a pressure pulsation spectrum diagram of the high pressure outlet of the energy recovery device under different structural designs at n = 1,200 rpm. As can be seen from Fig. 10, the structure *c* (double layer, area = 2,125.55 mm^2) has the largest peak amplitude at frequencies of 10 and 20 Hz. Structure *b* (single layer, area = 2,591.81 mm^2), followed by the peak amplitude, at a frequency of 20 Hz. Three kinds of structural design, high pressure inlet pressure fluctuation spectrum have certain periodicity. Among them, structure *a* (single layer, area = 3,534.29mm^2) has the lowest peak amplitude on the whole, and the amplitude fluctuation at the outlet is particularly small, which again shows that the end cover rotor area does have an impact on the stability of the desalination energy recovery device. The reasonable design of the end cover rotor area of the desalination energy recovery device can reduce the gap between the end cover and the rotor sealing surface dynamic and static interference can improve system stability and pressure energy recovery efficiency.

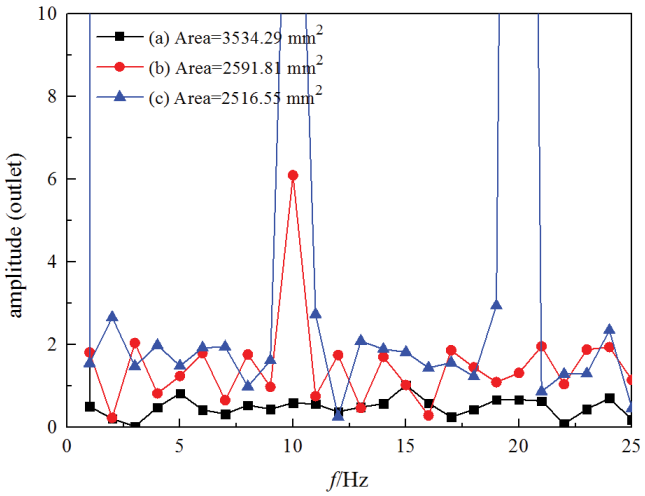

Fig. 10. n = 1,200 rpm, frequency spectrum of pressure fluctuation at high pressure outlet under different structures.

3.5. Internal concentration distribution of energy recovery unit

Through the analysis of energy recovery efficiency in section 3.1 (Pressure energy recovery efficiency), it is found that the effect of rotational speed on energy recovery efficiency mainly occurs at rotor speed n = 1,200; 1,400 rpm, and n = 1,200 rpm is the lowest efficiency point at the turning point of energy recovery efficiency of three structural design methods. Therefore, this paper focuses on the analysis of three-dimensional flow field pressure distribution in the energy recovery device when the rotate speed of the three structures is n = 1,200 rpm. Based on the analysis in section 3.4 (Energy recovery device high pressure inlet and outlet pressure pulsation), we found that the time and frequency domain characteristics of the high-pressure inlet and outlet pressures of the energy recovery device are periodic. Therefore, after analyzing the stable operation of the energy recovery device (the time step = 1 s), the effect of energy recovery efficiency can be explained by the effect of concentration on the efficiency of the energy recovery device when n = 1,200 rpm.

Fig. 11 depicts the concentration distribution of NaCl in the rotor of the desalination energy recovery unit when n = 1,200 rpm. From this figure, the desalination energy recovery device can realize pressure energy exchange under the three structural design, but the distribution of high and low concentration brine in the rotor is not the same. Structural *b* (single layer, area = 3,534.29mm^2) has the longest high concentration brine at a low pressure outlet, which indicates that the efficiency of the energy recovery device is related to the flow length of high concentration brine in the rotor. Combining with Fig. 4, it can be noted that the longer the flow length, the lower the efficiency.

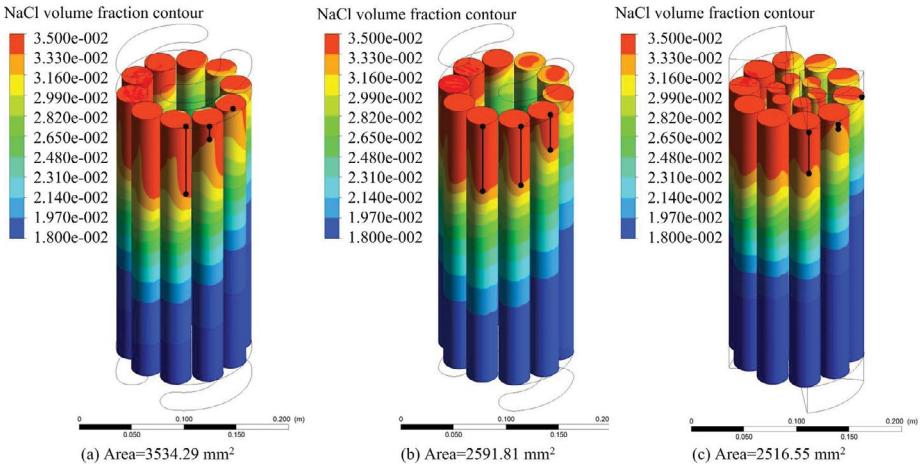

Fig. 11. Distribution of NaCl concentration in energy recovery device.

4. Conclusion

In this paper, CFD method is utilized to simulate the influence of the inner cover of the seawater desalination energy recovery device on the flow field characteristics and the pressure energy exchange efficiency under the three structural design. The results show that given the design flow rate Q, the influence of structural design form on pressure energy transfer is mainly as follows:

- The area of the end cover rotor plays an important role in the efficiency of pressure energy recovery. Unreasonable coverage area makes the efficiency of pressure energy recovery very low, which can not meet the design requirements. At the same time, the influence of rotating speed on the efficiency of pressure energy recovery is not unique, but there is a rotating speed that does not adapt to the efficiency of energy recovery. The greater the pressure difference between the high pressure inlet and outlet of the energy recovery device, the lower the efficiency of pressure energy recovery (conversion). Reducing the pressure loss at the high pressure inlet and outlet is the key technology to improve the pressure energy recovery (conversion) efficiency of the energy recovery device.
- There is relative movement between the end cover and the rotor of the energy recovery device, so it is necessary to consider the formation of hydrostatic mechanical seal with fluid. Through the analysis of the time-domain and frequency-domain characteristics of the pressure fluctuation at the high-pressure inlet and outlet, the design method of structure *a* (single layer, area = 3,534.29 mm^2) and end cover covering the rotor area can reduce the static and dynamic interference between the end cover and the rotor sealing surface, improve the system stability and the efficiency of pressure energy recovery, which is the optimal design among the three structures.
- Under the three structural designs, the desalination energy recovery device can achieve pressure energy exchange, but the distribution of high and low concentration brine in the rotor channel is not the same. The efficiency of the energy recovery device is related to the flow length of high concentration brine in the rotor channel. The longer the flow length, the lower the efficiency.
- This characteristic occurs at n = 1,200 rpm, which shows that model c has a beneficial effect at this speed, but the speed is not the optimal model as a whole. Three models are selected to study the influence of the rotor area covered by the end cover on the energy recovery device. Through research and analysis, type c has the worst shortcomings and is not suitable for engineering application, which is also the conclusion of this numerical simulation study.

References

[1] E.L. Xu, G.M. Wang, M.D. Fan, L.F. Xie, Research progress of the rotary energy recovery device, Mem. Sci. Thec., 3 (2018) 144–151.

[2] A. Gary, N. Ghaffou, Z. Li, L. Francis, R.V. Linares, T. Missimer, S. Lattemann, Membrane-based seawater desalination: present and future prospects, Desalination, 401 (2017) 16–21.

[3] W.J.L. Misdan, A.F. Ismall, Seawater reverse osmosis (SWRO) desalination by thin film composite membrane – current development, challenges and future prospects, Desalination, 287 (2012) 228–237.

[4] A. Subramani, M. Badruzzaman, J. Oppenheimer, J.G. Jacangelo, Energy minimization strategies and renewable energy utilization for desalination: a review, Water Res., 45 (2011) 1907–1920.

[5] A. Belila, J. El-Chakhtoura, N. Otaibi, G. Gonzalez, G. Muyzer, M.C.M. van Loosdrecht, J.S. Vrouwenvelder, Bacterial community structure and variation in a full-scale seawater desalination plant for drinking water production, Water Res., 94 (2016) 62–72.

[6] A. Rodríguez-calvo, G.A. Silva-Castro, F. Osorio, J. Rodríguez-Calvo, C. Calvo, Reverse osmosis seawater desalination: current status of membrane systems, Desal. Water Treat., 4 (2015) 849–861.

[7] A.M. Bilton, L.C. Kelley, Design of power systems for reverse osmosis desalination in remote communities, Desal. Water Treat., 55 (2014) 2868–2883.

[8] L. Li, Key Structure Design and Mechanical Characteristics Analysis of Energy Recovery and Pressurization Unit for Seawater Desalination, Zhejiang University, Hangzhou, 2018.

[9] J.P. Macharg, Retro-fitting existing SWRO systems with a new energy recovery device, Desalination, 1 (2003) 253–264.

[10] Y.H. Zhou, X.W. Ding, M.W. Ju, Y.Q. Chang, Numerical simulation on a dynamic mixing process in ducts of a rotary pressure exchanger for SWRO, Desal. Water Treat., 1 (2012) 107–113.

[11] R. Stover, J. Martin, Titan PX-1200 energy recovery device – test results from the Inima Los Cabos, Mexico, seawater RO facility, Desal. Water Treat., 3 (2009) 179–182.

[12] L.P. Yang, H.W. Hu, B. Zhang, T. Shen, Simulation of chemical desorption of CO_2 in multi-effect distillation desalination system, CIESC J., 64 (2013) 956–964.

[13] E.L. Xu, Y. Wang, J. Zhou, S.C. Xu, S.C. Wang, Theoretical investigations on rotor speed of the self-driven rotary energy recovery device through CFD simulation, Desalination, 398 (2016) 189–197.

[14] E. Dimitriou, E.S. Mohamed, C. Karavas, G. Papadakis, Experimental comparison of the performance of two reverse osmosis desalination units equipped with different energy recovery devices, Desal. Water Treat., 55 (2015) 3019–3026.

[15] B.Y. Li, J.Y. Wang, J.H. Wang, H.B. Liu, Modeling and optimization of hollow fiber air gap membrane distillation for seawater desalination, CIESC J., 2 (2015) 596–605.

[16] B.A. Qureshi, S.M. Zubair, Exergetic analysis of a brackish water reverse osmosis desalination unit with various energy recovery systems, Energy, 93 (2015) 256–265.

[17] N. Liu, Z.L. Liu, Y.X. Li, L.X. Sang, Studies on leakage characteristics and efficiency of a fully-rotary valve energy recovery device by CFD simulation, Desalination, 415 (2017) 40–48.

[18] B.W. Qi, Y. Wang, Z.C. Wang, Y.P. Zhang, S.C. Xu, S.C. Wang, Theoretical investigation on internal leakage and its effect on the efficiency of fluid switcher-energy recovery device for reverse osmosis desalting plant, Chin. J. Chem. Eng., 11 (2013) 1216–1223.

[19] M. Nikolay, S. Ilya, P. Anton, D. Kratirov, K. Levin, Cyclone separator for gas-liquid mixture with high flux density, Powder Technol., 339 (2018) 326–333.

[20] F. Jiang, P. Huang, Fluent Advanced Application and Case Study, Tsinghua University Press, Beijing, 2008.

[21] J.Y. Tao, Z. Lin, C.J. Ma, J.H. Ye, Z.C. Zhu, Y. Li, Mao, W. Mao, An experimental and numerical study of regulating performance and flow loss in the V-port ball valve, J. Fluids Eng., 142 (2020) 2071–2079.

[22] H.J. Zhu, Y.H. Lin, L.H. Xie, Fluent Fluid Analysis and Simulation Practical Course, People's Posts and Telecommunications Press, Beijing, 2010.

[23] Z. Wen, L.C. Shi, Y.R. Ren, Fluent Fluid Computing Application Course, Tsinghua University Press, Beijing, 2009.

[24] R.L. Stover, Development of a fourth generation energy recovery device, A 'CTO's notebook', Desalination, 165 (2004) 313–321.